

# A Potential Interaction Between E2F-1 and Akt1 Resulting in CDDP-Induced Apoptosis in Triple Negative Breast Cancer Cell Line

Samiya Al-Jaaidi<sup>1\*</sup>, Buthaina Al-Dhahli<sup>2</sup>, Asma Al Sibani<sup>3</sup>, Thraia Al Harthi<sup>4</sup>, Hajar Al Ghafri<sup>5</sup> and Shadia Al-Bahlani<sup>2</sup>

<sup>1</sup>Department of Biology, College of Science, Sultan Qaboos University, Oman

<sup>2</sup> Department of Biomedical Science, College of Medicine and Health Sciences, Sultan Qaboos University, Oman

<sup>3</sup>Sultan Qaboos Comprehensive Cancer Care and Research Center, University Medical City, Oman

<sup>4</sup>Ibra health centre laboratory, Ministry of Health, Oman

<sup>5</sup>Department of Microbiology and Immunology, Sultan Qaboos University Hospital, University Medical City, Oman

*Received: 5 June 2024*

*Accepted: 23 October 2024*

\*Corresponding author: [bahlani@squ.edu.om](mailto:bahlani@squ.edu.om)

DOI 10.5001/omj.2025.41

## ***Abstract***

**Objectives:** We aimed to investigate the expression levels and interaction between E2F-1 and Akt1 which have not been studied in TNBC cells and whether CDDP could influence such an interaction.

**Methods:** MDA-MB-321 cells were treated with increasing concentrations of CDDP (2.5-40  $\mu$ M; 24 h). CDDP-induced apoptosis was confirmed biochemically using cleaved PARP and flow cytometry analysis and morphologically using Haematoxylin and Eosin staining, Hoechst stain and Scanning Electron Microscope. Caspase-3 cleavage, an indicator of apoptotic induction, was measured by immunofluorescence. Western blot was used to investigate the effect of CDDP on E2F-1 and Akt1 expression while their co-localization and interaction were detected using immunofluorescence and immunoprecipitation respectively.

**Results:** Western blot analysis revealed an increase in E2F-1 and a decrease in Akt1 expression as the concentration of CDDP increased compared to untreated cells. The merge of E2F-1 and Akt1 immunosignals observed by immunofluorescence demonstrated that CDDP-treated cells resulted in the co-localization of immunosignals in clusters and with increased intensity in the cytoplasm. Immunoprecipitation and western blot analysis further supported the interaction between E2F-1 and Akt1 indicating a potential interaction of both proteins at the endogenous level of MDA-MB-231 cells.

**Conclusions:** Our findings suggest a potential interaction between E2F-1 and Akt1 and that this interaction could be the precursor for the CDDP-induced apoptosis in TNBC cells. Further studies are needed to determine whether such interaction is directly or via an intermediate protein.

**Keywords:** E2F-1; Akt1; CDDP; TNBC; Interaction.

## **Introduction**

In females, breast cancer still remains the first most commonly diagnosed cancer (11.6%) and the leading cause of cancer death (6.9%) of all total cancers worldwide as reported by the WHO in 2022.<sup>1</sup> Breast cancers are sub-typed based on the expression of estrogen receptors (ER), progesterone receptors (PR) and human epidermal growth factor receptor-2 (HER-2) which provide key targets for drug therapy. Breast cancers that lack all these three types of receptors are called triple negative breast cancers (TNBC). Due to this, there are currently no

targeted treatments for TNBC.<sup>2</sup> One of the strategies used to address the treatment of TNBC are platinum-based chemotherapeutics such as Cis-diamminedichloroplatinum(II) (CDDP).<sup>3</sup> Although only a subset of TNBC patients are sensitive to CDDP, however, its anticancer effects are limited due to chemo-resistance leading to therapeutic failure.<sup>4</sup> A considerable effort has been made in understanding the molecular pathways that are implicated in TNBC resistance to chemotherapy. We and other groups have shown that TNBC cells can become resistant to CDDP by several mechanisms including repair of the DNA by excision repair mechanisms or via the deregulation of pro-apoptotic or anti-apoptotic proteins of the cell cycle.<sup>4-7</sup> Targeting deregulated apoptosis to relief sustained proliferation of TNBC cells from cell cycle progression represents an attractive approach to overcome chemotherapy resistance. Two of the key proteins that play an important role in the cell cycle and apoptosis are frequently activated/deregulated in human cancer are E2F-1 and Akt1.

E2F-1, a member of a group of eight transcription factors, is unique in that it regulates cell cycle progression in normal cells but signals apoptosis in response to DNA damage.<sup>8</sup> E2F-1-induced apoptosis in response to DNA-damaging agents can be both dependent<sup>9</sup> and independent of p53.<sup>10</sup> E2F-1 has been found to be deregulated in many types of cancers including breast cancer cells.<sup>10-12</sup> Once recognized in its ability to chemosensitize cancer cells, deregulated E2F-1 can lose its apoptotic ability in late stage cancers and instead promote tumor invasion and metastasis mediating chemoresistance.<sup>13</sup>

Akt1, a serine threonine kinase, is one of the three isoforms of the Akt family. Akt also known as protein kinase B (PKB) is a key element of the phosphoinositide-3-kinase (PI3K)/Akt signalling pathway involved in the many aspects of cancer pathophysiology including tumor growth, survival and invasiveness.<sup>14</sup> Breast cancer is the most common cancer that shows alterations in the PI3K/Akt signalling pathway<sup>15</sup> and resistance to chemotherapy.<sup>16</sup> The three AKT isoforms, Akt1, Akt2 and Akt3, share high sequence and structural homology but elicit cell and context-specific effects.<sup>17</sup> Therefore, targeting Akt-isoform specific signalling in cancer is crucial to determine effective targeted therapies. In breast cancer, Akt-1 accelerates cell proliferation but suppresses metastasis.<sup>16,17</sup>

Limited studies have suggested the closely regulated relationship between E2F-1 and Akt. Hallstrom *et al.* (2008) reported that during the course of normal cellular proliferation, Akt protein kinase specifically blocks expression of genes in the E2F-1 apoptotic programme. They concluded that the E2F and Akt connection could explain why normal cycling cells do not die each time they transit through G1 to S phase of the cell cycle.<sup>18</sup> Chaussipied and Ginsberg (2004) reported that a negative feedback loop exists between E2F and Akt in malignant melanoma cells. E2F-1 upregulates Akt activity through Gab2, and the sustained E2F-1/Gab2/Akt pathway in turn inhibits E2F-1 via TopBp1 preventing E2F-1 from exerting its pro-apoptotic functions.<sup>19</sup> These studies reveal a crosstalk between E2F-1 and Akt, suggesting the existence of a dynamic relationship between cytoplasmic and nuclear signalling cascades. To date, there are no previous studies conducted to investigate both E2F-1 and Akt1 interaction in the context of CDDP sensitivity in TNBC. Therefore, this study aims to detect E2F-1 and Akt1 interaction and determine if their interaction influences TNBC sensitivity to CDDP-induced apoptosis.

## Methods

DMEM media, fetal bovine serum and 1% anti-biotic anti-mycotic solution were obtained from Gibco, Thermo Fisher Scientific, UK. CDDP (50 mg/50 mL) was obtained from Hospira, USA. FlowCollect Annexin Red Kit was obtained from Millipore, Germany. Hoechst 33258 dye (6.25 ng/mL) was purchased from SIGMA, Germany. Anti-mouse E2F-1 (ab135251) was obtained from abcam, USA. Anti-rabbit Akt1 (4685S) was obtained from cell signaling technology, USA. Anti-GAPDH (AM1020a) was bought from ABGent, USA. Anti-PARP (9542) was obtained from cell signaling technology, USA. West Dura detection kit was obtained from ThermoScientific, UK. Fluorescein-conjugated secondary antibodies were obtained from Fisher Scientific, UK. Protein G agarose beads were provided by cell signaling technology, US. Osmium tetroxide (OsO<sub>4</sub>) was obtained from Agar Scientific, UK. Hexamethyldisilazine (HMDS) was obtained from SIGMA-ALDRICH, USA.

At first, the MDA-MB-231 cell line was purchased from the Pasteur institute of Iran and has been used earlier.<sup>20</sup> Once received, the cell line was maintained in DMEM media supplemented with 10% fetal bovine serum and 1% anti-biotic anti-mycotic solution (all from Gibco, Thermo Fisher Scientific, UK). Then, the cells were maintained at 37 °C with a humidified 5% carbon dioxide atmosphere.

FlowCollect Annexin Red Kit (Millipore, Germany) was used to quantify alive and apoptotic MDA-MB-231 cells after treatment with CDDP. Briefly, cells were prepared in an assay buffer at a volume of 100 µL and pipetted into appropriate wells, to which 100 µL of Annexin V working solution were added. Cells were then incubated at

37°C for 15 minutes. Following incubation, 5 µL of 7-Aminoactinomycin D (7-AAD) were added per well. After incubation, they were incubated in the dark at room temperature for 5 minutes. Finally, acquisition and analysis were performed using guava HT System (guava easyCyte HT) with guava software.

Both alive and apoptotic MDA-MB-231 cells were determined by morphological features using Hoechst 33258 dye (6.25 ng/mL) (SIGMA, Germany), as described previously.<sup>20</sup> At least 400 cells per treatment group were selected blindly and counted randomly. Finally, they were visualized using Nikon ECLIPSE Ti-BTV2 fluorescent microscope.

Protein extraction and western blot were performed as described.<sup>20</sup> Briefly, membranes were incubated overnight at 4 °C with primary antibodies, and detected with horseradish peroxidase-conjugated goat IgG raised against the corresponding species (cell signaling technology, USA). Subsequently, Peroxidase activity was visualized with an enhanced chemiluminescence (ECL) kit (West Dura detection kit, ThermoScientific, UK). The signal was captured using GBox machine with GeneSys software. Finally, signal intensity was determined densitometrically using Image J software, version 1.47, (National Institute of Health, USA).

Cells grown on 12-well glass slides were treated with graded concentrations of CDDP (0, 20, and 40 µM) for 24 hours. Immunofluorescence staining was applied as previously described.<sup>7</sup> Briefly, cells were fixed by pre-cooled (-20°C) methanol for 3 minutes. Then, the cells were permeabilized for 5 minutes with 0.05% Triton X-100. After washing with Phosphate-Buffered Saline (PBS), cells were blocked with 1% Bovine Serum Albumin (BSA) for 30 minutes at 4 °C, washed again and incubated with (1:100) primary antibodies (cell signaling technology, USA) for 1 hour at room temperature. After PBS wash, fluorescein-conjugated secondary antibodies (Fisher Scientific, UK) were added (1:400) for 1 hour at room temperature. The PBS washing was performed before mounting. Imaging was performed using a Nikon ECLIPSE fluorescence microscope. Images were captured at 20x magnification and the fluorescence intensity of each protein for each group was determined per cell number in a selected field using image-J software. The shown compartments were the cytoplasm and the nucleus of each cell. The merged images were automatically generated by channel merge option in the Nikon NIS Element software. The acquired images of Akt1 and E2F1 were merged together to create an overlay. The overlay of the red fluorescent color (E2F1) and the green fluorescent color (Akt1) produced the yellowish to orangish fluorescent color that represent the co-localization of both proteins. After obtaining the merged image, the intensity of 100 cells in each treatment was obtained using image J software.

After treatment of MDA-MB-231 with CDDP, protein of interest was immunoprecipitated as previously described.<sup>7</sup> Briefly, protein lysate were pre-cleared by incubation with 20 µL of protein G agarose bead and 1 µg of goat monoclonal IgG antibody for 1 hour at 4°C (all from cell signaling technology, US). Then, centrifugation was performed at 3600×g for 1 minute. Pre-cleared supernatant was incubated with 20 µL of agarose beads and 1 µg of anti-E2F-1 rabbit monoclonal antibody or rabbit IgG isotype, overnight at 4 °C. Five washing with lysis buffer was performed before adding SDS-loading buffer. The precipitated proteins were detected by western blot as described above.

MDA-MB-231 cells seeded in 12-well slide and treated with CDDP were fixed by 10% neutral buffered formalin for 30 minutes. Then cells were re-hydrated through graded alcohols. After washing with distilled water, Haematoxyline stain was added for 10 minutes. Differentiation was in 1% acid alcohol for few dips. Washing in running tap water for 5 minutes was followed by adding 1% Eosin solution for 4 minutes. Cells were rapidly dehydrated and cleared and then mounted with distyrene polystyrene xylene (DPX)

Cells cultured in cover-slips and treated with CDDP, to be visualized by SEM as described previously.<sup>6</sup> Briefly, cells were fixed in 2.5% glutaraldehyde in sodium cacodylate buffer (1 M, pH 7.3) for 10 minutes. After washing with 1 M sodium cacodylate for 2 minutes, 1% Osmium tetroxide (OsO<sub>4</sub>) (Agar Scientific, UK) was used to postfix the cells for 5 minutes followed by rapid wash in distilled water. Then cells were dehydrated in ethanol series (25%, 50%, 70%, 95%, 100%), 1 minute in each and dried subsequently using Hexamethyldisilazine (HMDS) (SIGMA-ALDRICH, USA). Following that, they were mounted on aluminum stubs and coated with gold particles to prevent electrical charge effects. Cells were scanned using Scanning Electron Microscope JEOL JSM-5600LV.

Means and standard deviation were calculated and analyzed by independent t-test or single-factor analysis of variance (One-way ANOVA) using SSPS and Microsoft Excel. All measurements were considered significant if *p*-value is <0.05.

The authors declare no ethical approval is required as only commercial secondary cell lines were used.

## Results

Both biochemical and morphological aspects of apoptosis were studied in MDA-MB-231 cells after their pretreatment with CDDP. Different concentrations were used to determine the optimum dose of CDDP that can produce significant apoptosis without reaching cytotoxicity.<sup>21</sup> As shown in Figure 1b, 24 hours exposure to varying concentrations of CDDP at 10, 20 and 40  $\mu\text{M}$  resulted in a significant dose-dependent increase in apoptosis in comparison to untreated cells. To determine whether CDDP-induced cytotoxicity was due to the induction of apoptosis in MDA-MB-231 cells, the level of associated apoptotic protein, PARP, was detected by western blot. PARP, a DNA binding enzyme that can detect DNA strand breaks, is a substrate that is cleaved by both caspase-3 and caspase-7.<sup>22</sup> The presence of cleaved PARP is used as a diagnostic test to detect apoptosis in many cell types.<sup>22</sup> As shown by western blot in Figure 1a, PARP cleavage showed that the PARP protein was degraded, generating a concomitant diminution of full size (116 KD) molecule and accumulation of the 85 KD in MDA-MB-231 cells treated with CDDP at 20 and 40  $\mu\text{M}$  after 24 hours. These results provide strong evidence that apoptosis was induced in CDDP-treated cells.

To further confirm that CDDP induces apoptosis in MDA-MB-231 cells, flow cytometry analysis with Annexin V-FITC and 7-AAD double staining was used. Figure 1c indicates that MDA-MB-231 cells treated with CDDP at 20  $\mu\text{M}$  for 24 hours presented with approximately 20% apoptosis.

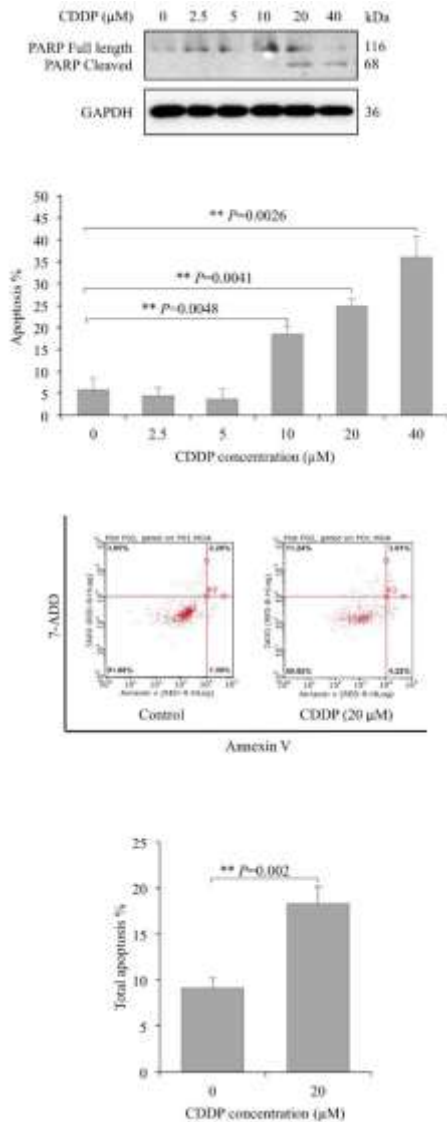


**Figure 1:** CDDP induced apoptosis in a concentration-dependent manner in MDA-MB-231 cells. (a) The effect of CDDP on PARP expression (full length and cleaved) in MDA-MB-231 cells analyzed by western blot. (b) Graphical presentation of estimated apoptosis percentage by Hoechst stain method in MDA-MB-231 cells treated with different concentrations of CDDP showing significant increase in apoptosis in comparison to the control (\* $P < 0.05$ , \*\* $P < 0.01$ , \*\*\* $P < 0.001$ ). (c) Dot graphs and graphical presentation show flow-cytometric analysis of apoptosis following treatment of MDA-MB-231 cells with CDDP. Bar graphs show significant increase in apoptosis in comparison to control concentration (\* $P < 0.05$ , \*\* $P < 0.01$ , \*\*\* $P < 0.001$ ).

Three experimental techniques were used to detect and characterize the morphology of MDA-MB-231 cells in response to CDDP-induced apoptosis. As shown in Figure 2, Hoechst staining, which correlated with the presence of cells with typical apoptotic nuclear morphology (pyknotic and fragmented nuclei), was present in the cells treated with 20  $\mu\text{M}$  for 24 hours, but not in the untreated cells.

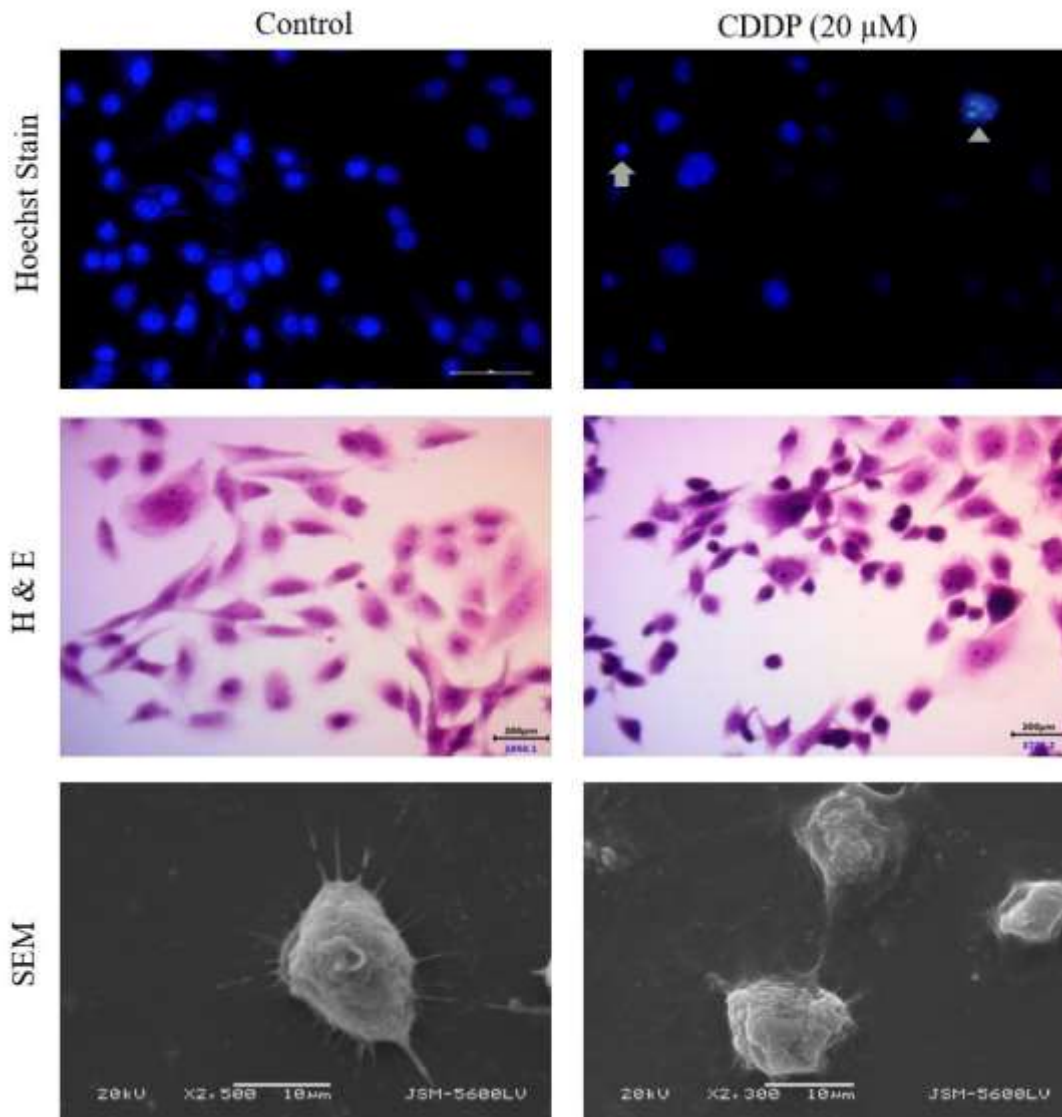


**Figure 2:** CDDP caused morphological changes in MDA-MB-231 cells. Representative morphology of MDA-MB-231 cells following CDDP treatment. Hoechst-stained cells show apoptotic features, pyknotic (arrow) and fragmented (arrow head) nuclei compared to a live cell nucleus. Heamatoxylin and Eosin stained cells show shrinkage of cytoplasm and nuclear pyknosis compared to untreated cells. SEM micrographs of CDDP-treated cells with shrinkage of lamellipodia, surface pores and grooves compared to untreated cells. Images for Hoechst and Heamatoxylin and Eosin stains were captured at 40x magnification while for SEM micrograph was screened at 2-5 $\mu\text{M}$ .

To further examine morphological changes, the treated cells were stained with haematoxylin and eosin. Control cells exhibited normal shape of nuclei that were round, homogeneous and stained dark blue. In contrast, cells treated with 20  $\mu\text{M}$  for 24 hours exhibited typical characteristics of apoptosis, such as nuclear pyknosis and fragmentation that was stained dark blue, as shown in Figure 2.

The treated cells were also examined by SEM in order to reveal cell blebbing and fragmentation. At the concentration of 20  $\mu\text{M}$  of CDDP, SEM revealed shrunken and round-shaped cells with shrinkage of lamellipodia, membrane blebs and apoptotic bodies compared to untreated cells that showed higher numbers and thicker membrane-bound protrusions and lamellipodia as indicated in Figure 2.

Since the activation of caspases is a hallmark of apoptosis, the cellular compartmentalization of the cleaved nuclear protein, caspase-3, was assessed in MDA-MB-231 cells treated with 20  $\mu\text{M}$  of CDDP using immunofluorescence microscopy analysis. As shown in Figure 3, the 4',6-diamidino-2-phenylindole (DAPI) nuclear staining showed morphological changes in terms of both nuclear condensation and cell structure loss and significant expression of cleaved caspase-3 in treated cells compared to control cells. Altogether these results signify an indication of apoptotic activity of CDDP in MDA-MB-231 cells.

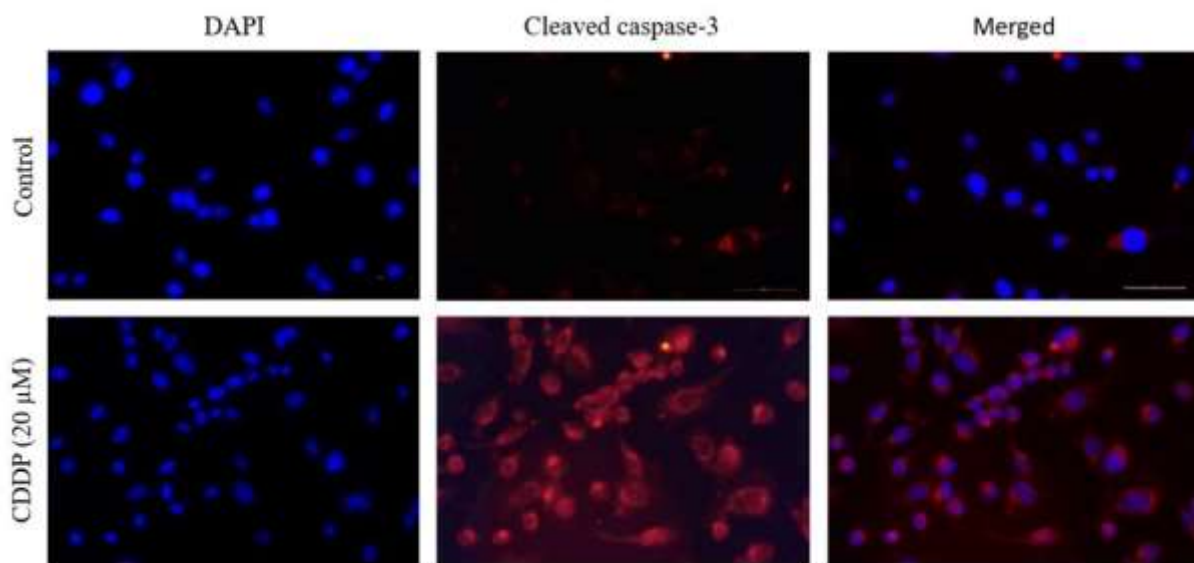


**Figure 3:** CDDP activated caspase-3 protein via its cleaved form in MDA-MB-231 cells. Immunofluorescence staining of cleaved caspase-3 in MDA-MB-231 cells following CDDP treatment show an increase in expression compared to untreated cells. The DAPI stain was used as a control for nuclear staining. All images were captured at 40x magnifications and the merged images were automatically generated by Imaging systems in fluorescence microscope. The shown compartments were the cytoplasm and the nucleus of each cell.

To determine whether CDDP has a differential effect on E2F-1 and Akt1 in MDA-MB-231 cells, the expression of these two proteins were investigated. Western blot revealed that the expression of E2F-1 contents increased and the expression of Akt1 decreased as the concentration of CDDP increased (20 and 40  $\mu\text{M}$ ; 24 h) compared to untreated cells.

The expression of E2F-1 and Akt-1 as demonstrated in the western blot led us to speculate that these two endogenous proteins may be co-localizing and interacting in MDA-MB-231 cells. To explore this possibility, E2F-1 and Akt-1 co-localization and interaction was examined in control and CDDP treated cells (20 and 40  $\mu\text{M}$ ; 24 hours) using immunofluorescence.

Immunofluorescence demonstrated that E2F-1 immunosignal was present in both the cytoplasm and the nucleus with approximately equal intensities. Akt1 immunoreactivity signals were mainly located in the cytoplasm compared to the nucleus. With CDDP treatment, E2F-1 immunoreactivity increased and became more localized in the nucleus in a concentration- dependent manner as presented in Figure 4. Conversely, CDDP had no effect on the localization of Akt1. The intensity of Akt1 immunosignal still remained high in the cytoplasm but a low

immunoreactivity in the nucleus was still detectable. The merge of E2F-1 and Akt1 immunosignals demonstrated that CDDP-treated cells resulted in the co-localization of immunosignals in clusters and with increased intensity in the cytoplasm. Thus, differential co-localization of both proteins in this cell line could be the precursor for the CDDP-induced apoptosis.

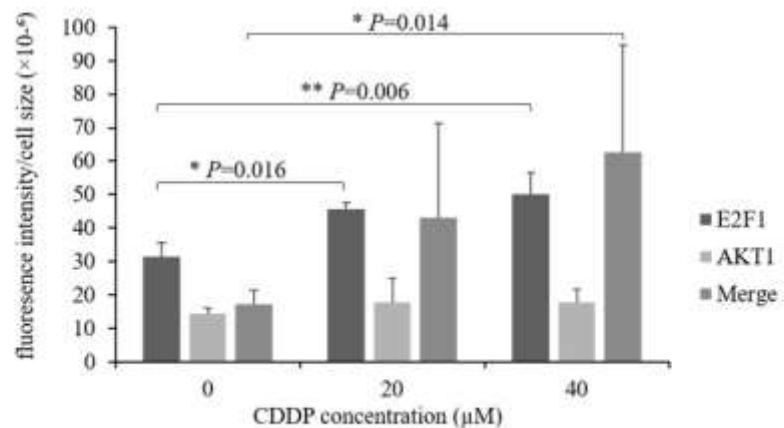
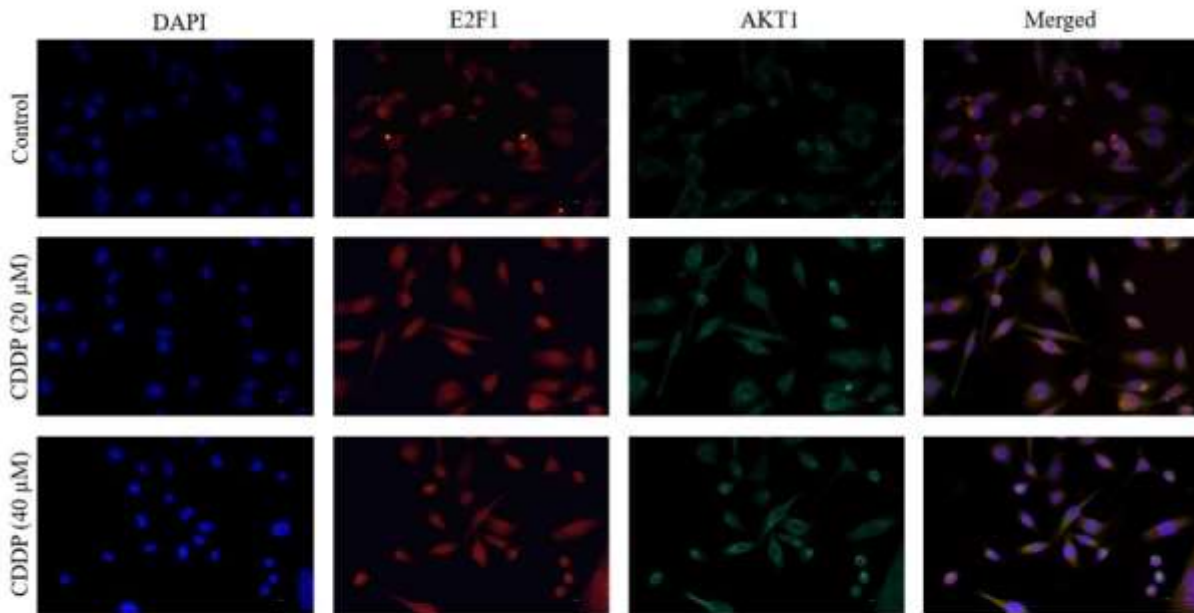


**Figure 4:** CDDP enhanced E2F-1 and Akt1 co-localization in MDA-MB-231 cells. (a) Immunofluorescence images demonstrate the effect of CDDP on co-localization and expression of E2F-1 and Akt1 in MDA-MB-231 cells. The cells were treated with different CDDP concentrations (0, 20, 40 μM). The fluorescence intensity of each protein for each group was determined per cell number in a selected field using image-J software. The shown compartments were the cytoplasm and the nucleus of each cell. DAPI stain was used as a control for nuclear staining. Images represent three independent experiments and they were captured at 40x magnifications and the merged images were automatically generated by Imaging systems in fluorescence microscope. (b) A scatter plot shows changes in estimated intensities of E2F-1, Akt1 and merged cells in MDA-MB-231 cells following CDDP treatment. E2F-1 intensity increased gradually while Akt1 intensity remained constant as CDDP dose increased (20 and 40 μM; 24 hours). The scattered dots represent the mean of ten cells per field counted from 10 fields per replicate for each treatment resulting in a total of 100 counted cells. Statistical analysis were obtained from three independent experiments using one way ANOVA (\*P<0.05, \*\*P<0.01, \*\*\*P<0.001).

To further validate the interaction of the two endogenous proteins, E2F-1 and Akt1 interaction was examined by immunoprecipitation. We chose to precipitate E2F-1 and detect the possible co-precipitation of Akt1 because CDDP increased its expression in these cells unlike Akt1 as indicated in Figure 5. Western blot revealed that Akt1 successfully co-precipitated with E2F-1 in both control and treated cells in a concentration-dependent manner indicating a potential interaction of both proteins at the endogenous level of MDA-MB-231 cells as seen in Figure 6.

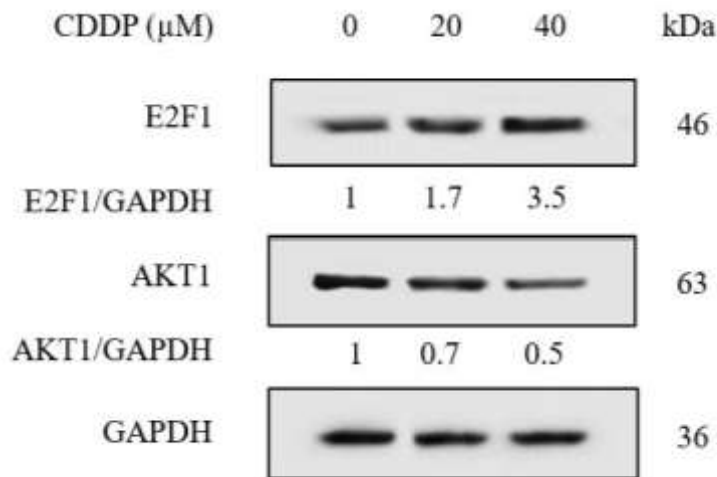


**Figure 5:** CDDP differentially affected E2F-1 and Akt1 expression in MDA-MB-231 cells. Immunoblotting reveals the expression of E2F1 and Akt1 proteins using specific antibodies after 24 hours treatment with different concentrations (20 and 40 μM) of CDDP. CDDP significantly increases E2F-1 expression while decreases Akt1 expression in a concentration dependent manner.

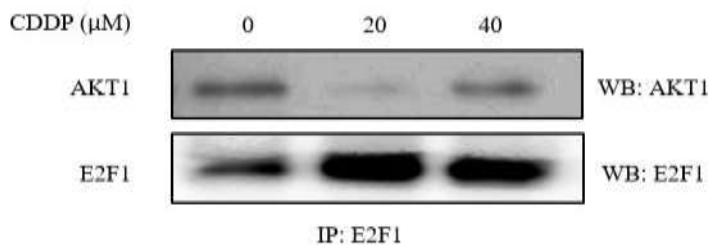


**Figure 6:** CDDP increased E2F-1 and Akt1 interaction in MDA-MB-231 cells. A western blot shows immunoprecipitation result. E2F-1 and Akt1 were successfully co-precipitated by anti-E2F-1 antibody in MDA-MB-231 cells treated with graded CDDP concentrations (20 and 40 μM; 24 hours). E2F1 and Akt1 binding was noticed in both controlled and treated groups in which, such binding was enhanced by the different concentrations of CDDP. The experiment was triplicated and the presented results are obtained from a representative replicate.

## Discussion

In this study, we demonstrated that MDA-MB-231 cells respond to CDDP treatment and that such a response is by induction of apoptosis. We then measured the expression levels of E2F1 and Akt1 when exposed to CDDP. We then examined the potential influence of CDDP on the interaction between E2F-1 and Akt1 in MDA-MB-231 cells and that this interaction likely activates apoptosis. To our knowledge, this is the first report, to examine the interaction between E2F-1 and Akt1 in CDDP-induced apoptosis in TNBC.

We have previously provided a full description of how platinum-based drugs affect the ultrastructure of breast cancer cell types using both SEM and TEM revealing apoptosis as the major mechanism for cell death.<sup>6</sup> These apoptotic findings are consistent with other studies in which apoptosis is evident in MDA-MB-231 cell line<sup>21,23,24</sup> and other cancer cell lines<sup>25-27</sup> following exposure to CDDP.

In this study, MDA-MB-231 cells were selected because; firstly, they represent the TNBC resistant cell line of the basal-like subtype which lack the three receptors (ER, PR and HER-2).<sup>28</sup> Secondly, this cell line is more difficult to treat due to lack of targeted therapy and therefore, generally has poor prognosis.<sup>29</sup> Thirdly, mutations in the p53 are observed in more than 50% of all human cancers<sup>30</sup> and MDA-MB-231 cells are known to harbour mutant p53.<sup>31</sup> Therefore, this provides the scientific rationale that CDDP induces apoptosis in a p53-independent pathway rendering these cells to possibly die in an E2F-1 apoptotic pathway as mutations in E2F-1 are very rare in cancer cells.<sup>32</sup> It is also suggested that E2F-1 may preferentially induce apoptosis in breast and ovarian cancer cells that have mutations in p53.<sup>11</sup> CDDP was selected because it is a potential treatment option for TNBC either alone or in combination with other drug agents.<sup>3</sup>

In this study, CDDP reproducibly induced apoptosis in a dose-dependent manner (10, 20 and 40  $\mu$ M; 24 h). Apoptosis was clearly detected by two distinct methods; biochemically and morphologically in MDA-MB-231 cells treated with 20  $\mu$ M dose of CDDP as this concentration effectively induced the cleavage of PARP. These results are in agreement with other studies that have shown that lower doses of CDDP (20 to 100  $\mu$ M range) result in apoptosis of MDA-MB-231 cells.<sup>23,24</sup> Apoptosis in 20  $\mu$ M CDDP treated cells was further confirmed biochemically by caspase-3 activation and flow cytometric analysis. The results of morphological studies using three different methods; Hoescht stain, Haematoxylin and Eosin stain and SEM altogether revealed and further validated the differential structural changes typical of apoptosis.

Given the role that E2F-1 is in cross-talk with the PI3-K /Akt pathway, it was of interest to evaluate whether a relationship exists between E2F-1 and Akt1 expression levels in response to CDDP and to detect their interaction in TNBC. We observed an inverse relationship between increased E2F-1 and decreased Akt1 expression levels in response to CDDP in a dose-dependent manner in this cell line. CDDP has been shown to induce a substantial increase of endogenous E2F-1 protein levels enhancing apoptosis in other cancer cell lines that lack p53.<sup>33</sup> Consistent with our observations, increasing concentration of CDDP (0.1 to 50  $\mu$ g/mL) was found to have no effect on Akt in MDA-MB-231 cells.<sup>34</sup> Since CDDP differentially affected E2F-1 and Akt1 protein expression levels suggests that an interaction between E2F-1 and Akt1 exists and that this interaction could be the precursor for the CDDP-induced apoptosis in TNBC. Exposure to CDDP had no effect on Akt1 localization, however, E2F-1 protein immunosignal intensity increased in the nucleus, a compartment consistent with its defined role in DNA repair.<sup>35</sup> Furthermore, an induced accumulation of E2F-1 protein by several DNA damaging chemotherapeutic drugs has been observed in a variety of tumor cell lines independent of p53 and pRb.<sup>36</sup> Interestingly, our results revealed here that the elevated intensity of both proteins in the cytoplasm in response to CDDP suggests that they are interacting in the cytoplasm. This is the first report detecting the subcellular localization and interaction between E2F-1 and Akt1 in TNBC exposed to CDDP. Consistent with other reports, Akt1 has been found to be located mainly in the cytoplasm in the MDA-MB-231 cell line and other cell lines that lack p53.<sup>37</sup> Ivanova *et al.* demonstrated that E2F-1 can shuttle into and out of the nucleus in a variety of cell types.<sup>38</sup> Yu *et al.* showed that CDDP cytotoxicity apart from inducing nuclear independent apoptosis, can be initiated by cytoplasmic events such as cytoplasmic cdk2 promoting apoptosis.<sup>39</sup> E2F-1 is one of the downstream components of Akt1<sup>19</sup> and E2F-1 nuclear-independent apoptotic functions in CDDP cytotoxicity have been described.<sup>40</sup> It is possible that the subcellular localization of E2F-1 at the cytoplasm and its potential interaction with Akt1 is a mechanism by which E2F-1 determines the cell fate to overcome chemoresistance. On the basis of the ability of anti-E2F-1 antibody to immunoprecipitate Akt1, it is evident that E2F-1 and Akt1 physically associate in TNBC.

## Conclusion

This study provides evidence of E2F-1 and Akt1 interaction through immunofluorescence by their co-localization in the cytoplasm in response to CDDP. In addition, the Immunoprecipitation demonstrated such interaction is involved in CDDP-induced apoptosis, thus aiding in the chemosensitivity of TNBC. Further exploration is needed in order to determine whether such interaction is directly or via an intermediate protein. It is also important to manipulate their expression to confirm that such interaction is required for CDDP to exert its effect in these cells.

## Disclosure

The authors declare no conflict of interest. The authors' contributions to this paper were as follows: SB: concept, design and supervision of the study, literature search, critical revision of the manuscript. SJ: manuscript preparation, literature search, critical analysis of the data. BD, AS, TH & HG: laboratory investigations and data collection. This work was funded by a grant from College of Medicine and Health Sciences, Sultan Qaboos University (Grant No. IG/MED/PATH/14/01).

## Acknowledgements

The authors thank staff in Electron Microscope Unit, Department of Pathology for expert technical assistance in SEM techniques.

## References

1. Bray F, Laversanne M, Sung H, Ferlay J, Siegel RL, Soerjomataram I, et al. Global cancer statistics 2022: GLOBOCAN estimates of incidence and mortality worldwide for 36 cancers in 185 countries. *CA Cancer J Clin* 2024;74(3):229-263.
2. Denkert C, Liedtke C, Tutt A, von Minckwitz G. Molecular alterations in triple-negative breast cancer-the road to new treatment strategies. *Lancet* 2017 Jun;389(10087):2430-2442. .
3. Jhan J-R, Andrechek ER. Triple-negative breast cancer and the potential for targeted therapy. *Pharmacogenomics* 2017 Nov;18(17):1595-1609.
4. Nedeljković M, Damjanović A. Mechanisms of Chemotherapy Resistance in Triple-Negative Breast Cancer-How We Can Rise to the Challenge. *Cells* 2019 Aug;8(9):957. . From NLM.
5. Galluzzi L, Senovilla L, Vitale I, Michels J, Martins I, Kepp O, et al. Molecular mechanisms of cisplatin resistance. *Oncogene* 2012 Apr;31(15):1869-1883. . From NLM.
6. Al-Bahlani S, Al-Dhahli B, Al-Adawi K, Al-Nabhani A, Al-Kindi M. Platinum-Based Drugs Differentially Affect the Ultrastructure of Breast Cancer Cell Types. *Biomed Res Int* 2017;2017:3178794. . From NLM.
7. Al-Bahlani S, Fraser M, Wong AY, Sayan BS, Bergeron R, Melino G, et al. P73 regulates cisplatin-induced apoptosis in ovarian cancer cells via a calcium/calpain-dependent mechanism. *Oncogene* 2011 Oct;30(41):4219-4230. . From NLM.
8. DeGregori J, Johnson DG. Distinct and Overlapping Roles for E2F Family Members in Transcription, Proliferation and Apoptosis. *Curr Mol Med* 2006 Nov;6(7):739-748. .
9. Wu X, Levine AJ. p53 and E2F-1 cooperate to mediate apoptosis. *Proc Natl Acad Sci U S A* 1994 Apr;91(9):3602-3606. .
10. Sun B, Wingate H, Swisher SG, Keyomarsi K, Hunt KK. Absence of pRb facilitates E2F1-induced apoptosis in breast cancer cells. *Cell Cycle* 2010 Mar;9(6):1122-1130. . From NLM.
11. Hunt KK, Deng J, Liu TJ, Wilson-Heiner M, Swisher SG, Clayman G, et al. Adenovirus-mediated overexpression of the transcription factor E2F-1 induces apoptosis in human breast and ovarian carcinoma cell lines and does not require p53. *Cancer Res* 1997 Nov;57(21):4722-4726. From NLM.
12. Meng P, Ghosh R. Transcription addiction: can we garner the Yin and Yang functions of E2F1 for cancer therapy? *Cell Death Dis* 2014 Aug;5(8):e1360. . From NLM.
13. Pützer BM, Engelmann D. E2F1 apoptosis counterattacked: evil strikes back. *Trends Mol Med* 2013 Feb;19(2):89-98. .
14. Cicenas J. The potential role of Akt phosphorylation in human cancers. *Int J Biol Markers* 2008;23(1):1-9. .
15. Massihnia D, Galvano A, Fanale D, Perez A, Castiglia M, Incorvaia L, et al. Triple negative breast cancer: shedding light onto the role of pi3k/akt/mtor pathway. *Oncotarget* 2016 Sep;7(37):60712-60722. . PubMed.
16. Li W, Hou JZ, Niu J, Xi ZQ, Ma C, Sun H, et al. Akt1 inhibition promotes breast cancer metastasis through EGFR-mediated  $\beta$ -catenin nuclear accumulation. *Cell Commun Signal* 2018 Nov;16(1):82. . From NLM.
17. Hinz N, Jücker M. Distinct functions of AKT isoforms in breast cancer: a comprehensive review. *Cell Commun Signal* 2019 Nov;17(1):154. .
18. Hallstrom TC, Mori S, Nevins JR. An E2F1-dependent gene expression program that determines the balance between proliferation and cell death. *Cancer Cell* 2008 Jan;13(1):11-22.
19. Chaussepied M, Ginsberg D. Transcriptional regulation of AKT activation by E2F. *Mol Cell* 2004 Dec;16(5):831-837. . From NLM.
20. Al-Bahlani S, Al-Lawati H, Al-Adawi M, Al-Abri N, Al-Dhahli B, Al-Adawi K. Fatty acid synthase regulates the chemosensitivity of breast cancer cells to cisplatin-induced apoptosis. *Apoptosis* 2017 Jun;22(6):865-876. .
21. Pauzi AZ, Yeap SK, Abu N, Lim KL, Omar AR, Aziz SA, et al. Combination of cisplatin and bromelain exerts synergistic cytotoxic effects against breast cancer cell line MDA-MB-231 in vitro. *Chin Med* 2016 Nov;11:46. . From NLM.

22. Bressenot A, Marchal S, Bezdetsnaya L, Garrier J, Guillemin F, Plénat F. Assessment of apoptosis by immunohistochemistry to active caspase-3, active caspase-7, or cleaved PARP in monolayer cells and spheroid and subcutaneous xenografts of human carcinoma. *J Histochem Cytochem* 2009 Apr;57(4):289-300.
23. Zhang Y, Wang L, Gao P, Sun Z, Li N, Lu Y, et al. ISL1 promotes cancer progression and inhibits cisplatin sensitivity in triple-negative breast cancer cells. *Int J Mol Med* 2018 Nov;42(5):2343-2352.
24. Li S, Li Q, Lü J, et al. Targeted Inhibition of miR-221/222 Promotes Cell Sensitivity to Cisplatin in Triple-Negative Breast Cancer MDA-MB-231 Cells. *Front Genet* 2019;•••:10.
25. Mandic A, Hansson J, Linder S, Shoshan MC. Cisplatin induces endoplasmic reticulum stress and nucleus-independent apoptotic signaling. *J Biol Chem* 2003 Mar;278(11):9100-9106.
26. Chen W, Yang Y, Chen B, Lu P, Zhan L, Yu Q, et al. MiR-136 targets E2F1 to reverse cisplatin chemosensitivity in glioma cells. *J Neurooncol* 2014 Oct;120(1):43-53.
27. Swift LH, Golsteyn RM. Cytotoxic amounts of cisplatin induce either checkpoint adaptation or apoptosis in a concentration-dependent manner in cancer cells. *Biol Cell* 2016 May;108(5):127-148.
28. Cailleau R, Young R, Olivé M, Reeves WJ Jr. Breast tumor cell lines from pleural effusions. *J Natl Cancer Inst* 1974 Sep;53(3):661-674.
29. Prabhakaran P, Hassiotou F, Blancafort P, Filgueira L. Cisplatin induces differentiation of breast cancer cells. *Front Oncol* 2013 Jun;3:134.
30. Hainaut P, Hollstein M. p53 and human cancer: the first ten thousand mutations. In *Advances in cancer research*, Vol. 77; Elsevier, 1999; pp 81-137.
31. Olivier M, Eeles R, Hollstein M, Khan MA, Harris CC, Hainaut P. The IARC TP53 database: new online mutation analysis and recommendations to users. *Hum Mutat* 2002 Jun;19(6):607-614.
32. Poppy Roworth A, Ghari F, La Thangue NB. To live or let die - complexity within the E2F1 pathway. *Mol Cell Oncol* 2015 Jan;2(1):e970480.
33. O'Connor DJ, Lu X. Stress signals induce transcriptionally inactive E2F-1 independently of p53 and Rb. *Oncogene* 2000 May;19(20):2369-2376. .
34. Johnson-Holiday C, Singh R, Johnson EL, Grizzle WE, Lillard JW Jr, Singh S. CCR9-CCL25 interactions promote cisplatin resistance in breast cancer cell through Akt activation in a PI3K-dependent and FAK-independent fashion. *World J Surg Oncol* 2011 May;9(1):46.
35. Guo R, Chen J, Zhu F, Biswas AK, Berton TR, Mitchell DL, et al. E2F1 localizes to sites of UV-induced DNA damage to enhance nucleotide excision repair. *J Biol Chem* 2010 Jun;285(25):19308-19315.
36. Lin W-C, Lin F-T, Nevins JR. Selective induction of E2F1 in response to DNA damage, mediated by ATM-dependent phosphorylation. *Genes Dev* 2001 Jul;15(14):1833-1844.
37. Santi SA, Lee H. The Akt isoforms are present at distinct subcellular locations. *Am J Physiol Cell Physiol* 2010 Mar;298(3):C580-C591.
38. Ivanova IA, Vespa A, Dagnino L. A novel mechanism of E2F1 regulation via nucleocytoplasmic shuttling: determinants of nuclear import and export. *Cell Cycle* 2007 Sep;6(17):2186-2195. .
39. Yu F, Megyesi J, Price PM. Cytoplasmic initiation of cisplatin cytotoxicity. *Am J Physiol Renal Physiol* 2008 Jul;295(1):F44-F52. . PubMed.
40. Bell LA, O'Prey J, Ryan KM. DNA-binding independent cell death from a minimal proapoptotic region of E2F-1. *Oncogene* 2006 Sep;25(41):5656-5663. .